

CRACK PROPAGATION IN POROELASTIC FLUID-SATURATED SOLIDS AT INTERSONIC VELOCITIES

B. Loret¹ and E. Radi²

¹ Institut de Mécanique de Grenoble, Laboratoire Sols Solides Structures, 38041 Grenoble, France

² Dipartimento di Scienze e Metodi dell'Ingegneria, Università di Modena e Reggio Emilia, 42100 Reggio Emilia, Italia

ABSTRACT

A closed-form solution is provided for the stress, pore pressure and displacement fields near the tip of a crack, steadily running in an elastic fluid-saturated porous solid at crack tip speed ranging between the faster longitudinal wave-speed and the lower between the longitudinal Biot second wave-speed and the shear wave-speed. Mode I and Mode II loading conditions with permeable crack surfaces have been considered. The Biot theory of poroelasticity with inertia forces is assumed to govern the motion of the medium. At variance with the subsonic case where the crack tip fields are continuous in the body, for intersonic crack propagation, the stress and pore pressure fields display a strong discontinuity (shock wave) across two or four symmetric rays emanating from the moving crack tip. The obtained solution also reveals that favorable velocity regimes, occurring with crack face displacements in agreement with the sign of the tractions ahead of the crack tip, exist under both Mode I and Mode II loading conditions. The singularity of the stress and pore pressure fields predicted for these favorable regimes turns out to be weaker than the square-root singularity which characterizes the subsonic case. The introduction of a finite length cohesive zone allows to obtain an energy release rate at the crack tip that does not vanish, unlike for a point size process zone.

1 INTRODUCTION

The analysis of the stress and deformation fields near the tip of a crack dynamically propagating at high crack tip speeds in porous, fluid-saturated materials is of importance in many geophysical, environmental and biomechanical problems. Previous analytical investigations of crack propagation in fluid-saturated poroelastic media show that under quasistatic conditions the region close to the crack tip is practically drained [1, 2], whereas if the crack-tip dynamically propagates at subsonic speed, i. e. smaller than any of the three elastic wave-speeds for a poroelastic material, the pore pressure displays the same square root singularity as the partial stresses in the solid skeleton [3]. It is worth recalling that, in poroelastic materials, three elastic body waves propagate, two longitudinal waves affecting both solid and fluid phases and one shear-wave affecting only the solid phase. The relative order of the wave-speeds is of interest. The longitudinal wave-speed c_1 is always the largest. The order of the second longitudinal wave-speed c_2 and shear wave-speed c_3 depends mainly on porosity. For high porosity level, the speed c_2 of the slowest longitudinal wave (also called Biot wave) turns out to be smaller than the speed c_3 of the elastic shear wave, whereas the reverse order holds for low porosity level. Moreover, subsonic *and* super-Rayleigh crack propagation is found to be forbidden [3], because it would occur with negative energy flow to the crack tip, which implies crack face contact or compressive normal tractions ahead of the crack tip, in agreement with the dynamic propagation of a crack in homogeneous, linear elastic solids [4-5]. Note that the Rayleigh wave in poroelastic materials depends on the permeability properties of the free surface. In particular, for non-dissipative materials, it has been also proved that the Rayleigh wave speed for impermeable surface is smaller than any of the three elastic wave-speeds, whereas the Rayleigh wave for permeable surfaces exists only for low porosity level, up to a critical value defined by the condition $c_R = c_2$, which occurs for $c_2 < c_3$.

The analyses of intersonic crack propagation in linear and isotropic elastic materials performed in the last three decades [6-9] found that the crack-tip can propagate at speed between the shear wave speed c_s and the longitudinal wave speed c_L , but only under Mode II loading conditions. In this case, the stress fields suffer infinite jumps across two symmetric rays emanating from the moving crack tip and the resultant stress singularity at the crack tip and along the singular rays is weaker than square root, thus yielding a vanishing energy release rate, except for the special intermediate crack tip velocity $\sqrt{2} c_s$. However, Broberg [6] showed that the introduction of a cohesive zone model extends the favorable range of velocity to the entire intersonic regime, removing the problem of vanishing energy release rate. Investigations on Mode I intersonic crack propagation in linear elastic materials [5, 9] indicate that energy is not absorbed by the crack tip but emanates from it, which is not possible on physical ground, unless the loading is applied directly at the crack tip.

In the present investigation the analysis performed in [3] for subsonic crack propagation in a poroelastic medium has been extended to intersonic crack tip speed c between the largest and the smallest of the three poroelastic wave speeds. An analytical approach different from that developed in [3] is required, due to the modification in the character of the governing differential equations, which from elliptic turn hyperbolic, allowing for the appearance of strong discontinuity rays (shock wave front) emanating from the crack tip. The field equations are formulated in terms of eigensolutions and their relative amplitudes are fixed by the boundary conditions. By using a complex variable approach, closed form solutions are obtained for the three distinct intersonic regimes, under Mode I and Mode II loading conditions for the case of permeable crack surfaces.

2 GOVERNING EQUATIONS

Neglecting body forces and convective acceleration, the balances of momentum in terms of the apparent stress in the solid phase $\boldsymbol{\sigma}^s$ and of the intrinsic pore pressure p give:

$$\operatorname{div} \boldsymbol{\sigma}^s = \rho^s \ddot{\mathbf{u}}^s + \xi (\dot{\mathbf{u}}^s - \dot{\mathbf{u}}^w), \quad \operatorname{div} (-n p \mathbf{I}) = \rho^w \ddot{\mathbf{u}}^w - \xi (\dot{\mathbf{u}}^s - \dot{\mathbf{u}}^w). \quad (1)$$

Here \mathbf{u}^s and \mathbf{u}^w are the displacement vectors of the solid and fluid phases, n is the constant and uniform porosity, ξ is a constant proportional to the inverse of the permeability, ρ^s and ρ^w are the apparent mass densities of the two phases, namely $\rho^s = (1 - n) \rho_s$ and $\rho^w = n \rho_w$ where ρ_s and ρ_w are the intrinsic mass densities of the solid constituent and fluid.

The stress and the pore pressure depend on the strains in the solid and fluid phases, through the following linear elastic constitutive equations:

$$\boldsymbol{\sigma}^s = 2\mu \operatorname{sym} \nabla \mathbf{u}^s + (\lambda^s \operatorname{div} \mathbf{u}^s + \lambda^{sw} \operatorname{div} \mathbf{u}^w) \mathbf{I}, \quad -n p = \lambda^{sw} \operatorname{div} \mathbf{u}^s + \lambda^w \operatorname{div} \mathbf{u}^w. \quad (2)$$

The four parameters λ^s , λ^{sw} , λ^w and μ define the elastic material response and can be related to the Biot parameters, as shown by Loret [10]. The total stress of the mixture is defined as the sum of the apparent stresses in the phases, namely $\boldsymbol{\sigma} = \boldsymbol{\sigma}^s - n p \mathbf{I}$.

The problem of a plane crack propagating at constant speed c along a rectilinear path in an infinite medium is considered (see Fig. 1a). A Cartesian coordinate system $(0, x_1, x_2, x_3)$ centered at the crack tip and moving with it towards the x_1 direction is considered, with the out-of-plane x_3 -axis along the straight crack front. A cohesive zone model with length L much smaller than the crack length is considered. Under steady-state conditions the material derivative of an arbitrary scalar field ϕ becomes $\dot{\phi} = -c \phi_{,1}$.

For a plane problem, the displacement vectors can be expressed through the Green-Lamé decomposition, by introducing the longitudinal and shear displacement potentials for

the solid, $\varphi^s(x_1, x_2, t)$ and $\psi^s(x_1, x_2, t)$, and for the fluid, $\varphi^w(x_1, x_2, t)$ and $\psi^w(x_1, x_2, t)$, namely

$$\mathbf{u}^s_1 = \varphi^s_{,1} + \psi^s_{,2}, \quad \mathbf{u}^s_2 = \varphi^s_{,2} - \psi^s_{,1}, \quad \mathbf{u}^w_1 = \varphi^w_{,1} + \psi^w_{,2}, \quad \mathbf{u}^w_2 = \varphi^w_{,2} - \psi^w_{,1}. \quad (3)$$

The introduction of (2) and (3) into eqns (1), by using the material derivative rule under steady-state conditions, results in two systems of PDEs, for the longitudinal potentials:

$$\begin{aligned} (2\mu + \lambda^s - \rho^s c^2) \varphi^s_{,11} + (2\mu + \lambda^s) \varphi^s_{,22} + \lambda^{sw} (\varphi^w_{,11} + \varphi^w_{,22}) + c \xi (\varphi^s - \varphi^w)_{,1} &= 0, \\ \lambda^{sw} (\varphi^s_{,11} + \varphi^s_{,22}) + (\lambda^w - \rho^w c^2) \varphi^w_{,11} + \lambda^w \varphi^w_{,22} - c \xi (\varphi^s - \varphi^w)_{,1} &= 0, \end{aligned} \quad (4)$$

and for the shear potentials:

$$(\mu - \rho^s c^2) \psi^s_{,11} + \mu \psi^s_{,22} + c \xi (\psi^s - \psi^w)_{,1} = 0, \quad \rho^w c^2 \psi^w_{,11} + c \xi (\psi^s - \psi^w)_{,1} = 0. \quad (5)$$

It is worth noting that eqns (4), involving the longitudinal potentials φ^s and φ^w , are coupled, as a consequence of the explicit coupling between the dilatation of the elastic solid skeleton and the pressure p in the pore fluid and also as a consequence of the diffusion phenomenon embodied in Darcy's law. Eqns (5), involving the shear potentials for the displacements of the solid and fluid phases, are coupled through diffusion only. Hence, the latter equations uncouple in the non-dissipative case, namely for $\xi = 0$.

From the constitutive relations (2), the stress in the solid phase and the pore pressure become, in terms of displacement potentials:

$$\begin{aligned} \sigma^s_{11} &= (2\mu + \lambda^s) \varphi^s_{,11} + \lambda^s \varphi^s_{,22} + \lambda^{sw} (\varphi^w_{,11} + \varphi^w_{,22}) + 2 \mu \psi^s_{,12}, \\ \sigma^s_{22} &= \lambda^s \varphi^s_{,11} + (2\mu + \lambda^s) \varphi^s_{,22} + \lambda^{sw} (\varphi^w_{,11} + \varphi^w_{,22}) - 2 \mu \psi^s_{,12}, \\ \sigma^s_{12} &= \mu (2 \varphi^s_{,12} + \psi^s_{,22} - \psi^s_{,11}), \\ -n p &= \lambda^{sw} (\varphi^s_{,11} + \varphi^s_{,22}) + \lambda^w (\varphi^w_{,11} + \varphi^w_{,22}). \end{aligned} \quad (6)$$

The displacement potentials introduced in eqns (3) are assumed in the form:

$$\varphi^J(x_1, x_2) = a^J \operatorname{Re}[F(x_1 + \Omega x_2)], \quad \psi^J(x_1, x_2) = b^J \operatorname{Im}[G(x_1 + \Lambda x_2)]. \quad (J = s, w) \quad (7)$$

where a^J and b^J are real constants and F and G are analytic functions with respect to their complex arguments, over the whole plane except on the crack faces. The scalars Ω and Λ , which are imaginary for subsonic crack propagation, may be real or imaginary for inter-sonic crack propagation. The squares of the speeds of propagation of the two longitudinal waves and of the single shear wave in poroelastic solids are defined as

$$\left. \begin{aligned} c_1^2 \\ c_2^2 \end{aligned} \right\} = \frac{c_s^2 + c_w^2}{2} \pm \sqrt{\left(\frac{c_s^2 - c_w^2}{2}\right)^2 + c_{sw}^4}, \quad c_3^2 = \frac{\mu}{\rho^s}, \quad (8)$$

where $c_s^2 = (2\mu + \lambda^s)/\rho^s$, $c_w^2 = \lambda^w/\rho^w$ and $c_{sw}^4 = (\lambda^{sw})^2/\rho^s \rho^w$. The variations of the poroelastic wave-speeds, c_1 , c_2 and c_3 , with the porosity n has been reported in Fig. 1b, together with the variations of the Rayleigh wave-speeds for permeable and impermeable surfaces, c_R^{per} and c_R^{imp} , obtained in [3] for a non-dissipative Berea sandstone, namely for $\xi = 0$. The three wave speeds define three distinct inter-sonic regimes, which are denoted by *i*), *ii*) and *iii*) in Fig. 1b. With respect to the relative order of the three poroelastic wave speeds, from (8) it may be observed that c_1 is always larger than c_2 and c_3 . Moreover, $c_2 > c_3$ for low porosity, e. g. for $n < 0.128$ in Berea sandstone (see Fig. 1), whereas $c_3 > c_2$ for higher porosity n .

As argued in [3], in a local analysis of the crack tip zone, the dissipative terms in eqns (4) and (5) give higher order contribution and thus can be neglected, formally setting $\xi = 0$. These terms derive from the diffusion phenomenon introduced by Darcy's law, and they asymptotically vanish, since, for rapid dynamic crack propagation, the diffusion of the pore fluid does not play a role at the crack tip. For $\xi = 0$, a substitution of (7)₁ into eqns (4) yields the following eigenvalues problem for the longitudinal and shear potentials:

$$\begin{bmatrix} (1 + \Omega^2)c_s^2 - c^2 & (1 + \Omega^2)\lambda^{sw}/\rho^s \\ (1 + \Omega^2)\lambda^{sw}/\rho^w & (1 + \Omega^2)c_w^2 - c^2 \end{bmatrix} \begin{bmatrix} a^s \\ a^w \end{bmatrix} = \mathbf{0}, \quad \begin{bmatrix} (1 + \Lambda^2)c_3^2 - c^2 & 0 \\ 0 & c^2 \end{bmatrix} \begin{bmatrix} b^s \\ b^w \end{bmatrix} = \mathbf{0}. \quad (9)$$

For non-trivial solutions of eqns (9) to exist, the determinants of the associated coefficient matrices must vanish. Their characteristic equations provide two distinct eigenvalues Ω_1 and Ω_2 for the dilatational potentials and a single eigenvalue $\Lambda = \Omega_3$ for the rotational potentials, where $\Omega_j^2 = c^2/c_j^2 - 1$, for $j = 1, 2, 3$. The corresponding longitudinal eigenmodes resulting from (9) are such that:

$$a_k^w = \frac{\rho^s}{\lambda^{sw}} (c_k^2 - c_s^2) a_k^s. \quad (k = 1, 2) \quad (10)$$

For the shear eigenmode $b^w = 0$, so that $\psi^w(x_1, x_2) = 0$, and b^s is arbitrary. Then, the displacement potentials (7) assume the form:

$$\begin{aligned} \varphi^s(x_1, x_2) &= \text{Re}[F_1(z_1)] + \text{Re}[F_2(z_2)], & \psi^s(x_1, x_2) &= \text{Im}[G(z_3)], \\ \varphi^w(x_1, x_2) &= \frac{\rho^s}{\lambda^{sw}} \{(c_1^2 - c_s^2) \text{Re}[F_1(z_1)] - (c_s^2 - c_2^2) \text{Re}[F_2(z_2)]\}, \end{aligned} \quad (11)$$

where $z_j = x_1 + \Omega_j x_2$, for $j = 1, 2, 3$, and the analytic functions $F_1(z_1)$, $F_2(z_2)$ and $G(z_3)$ embody the constants a_1^s , a_2^s and b^s , respectively. The eigenvalues Ω_j , for $j = 1, 2, 3$, turn out to be real or imaginary, depending on the considered range of variation for the crack tip speed c . In any case, let α_j denotes the modulus of the corresponding Ω_j , namely $\alpha_j = |1 - c^2/c_j^2|^{1/2}$. Note that for $c > c_2$ then Ω_2 is a real constant. In this case, let $\text{Re}[F_2(z_2)] = f(z_2)$ where f is a real function of the real variable z_2 . Similarly, for $c > c_3$ let $\text{Im}[G(z_3)] = g(z_3)$ where g is a real function of the real variable z_3 . Due to Mode I or Mode II symmetry conditions, it is sufficient to consider the upper half-plane $x_2 > 0$, where $f(z_2)$ and $g(z_3)$ denote two propagating waves with the front along the planes $x_1 + \alpha_k x_2 = 0$, for $k = 2, 3$ (see Fig. 1a).

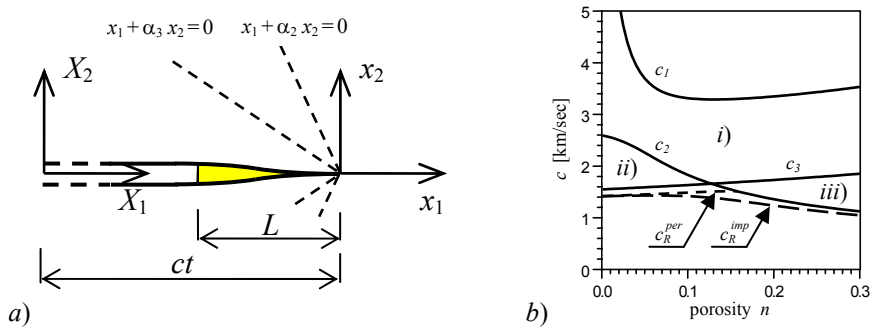


Figure 1. (a) geometry of the problem, with a cohesive zone of length L and two shock wave fronts, and (b) variations of poroelastic wave-speeds, c_1 , c_2 and c_3 , and Rayleigh wave-speeds, c_R^{per} and c_R^{imp} , with the porosity n , in Berea sandstone with $\xi = 0$.

Mode I loading conditions together with the conditions on the permeable crack surfaces and cohesive zone require

$$u_{2,1}^s(x_1, 0) = 0, \quad u_{2,1}^w(x_1, 0) = 0, \quad \text{for } x_1 > 0; \quad p(x_1, 0) = 0, \quad \text{for } x_1 < 0, \quad (12)$$

$$\sigma_{22}^s(x_1, 0) - n p(x_1, 0) = \begin{cases} \sigma(x_1) & \text{for } -L < x_1 < 0, \\ 0 & \text{for } x_1 < -L, \end{cases} \quad \sigma_{12}^s(x_1, 0) = 0, \quad \text{for all } x_1, \quad (13)$$

where $\sigma(x_1)$ denotes the normal stress distribution on the cohesive zone, having length L much smaller than the crack length. Similarly, under Mode II loading conditions

$$u_{1,1}^s(x_1, 0) = 0, \quad u_{1,1}^w(x_1, 0) = 0, \quad \text{for } x_1 > 0; \quad p(x_1, 0) = 0, \quad \text{for } x_1 < 0, \quad (14)$$

$$\sigma_{22}(x_1, 0) = 0, \quad \text{for all } x_1, \quad \sigma_{12}^s = \begin{cases} \tau(x_1) & \text{for } -L < x_1 < 0, \\ 0 & \text{for } x_1 < -L, \end{cases} \quad (15)$$

where $\tau(x_1)$ denotes the shear stress distribution on the cohesive zone.

3 RESULTS

Conditions (12)-(13) or (14)-(15) may be used to formulate an inhomogeneous Hilbert problem for the analytical function $F_1(z_1)$, which has been solved in closed form. The singularity of the stress and pore pressure fields near to the crack tip turns out to be different under Mode I or Mode II loading conditions. In particular, let $r^{-\gamma_1}$ and $r^{-\gamma_{II}}$ denote the asymptotic variations of these fields with the distance from the crack tip, then the performed investigations show that $\gamma_{II} = \gamma_1 \pm 1/2$. Note that intersonic crack propagation occurring with a stress and pore pressure singularity weaker than square-root turns out to be favorable, as it implies a positive energy release rate. Conversely, a stronger singularity is associated to non favorable conditions. Note that the introduction of a finite length cohesive zone yields a finite energy release rate at the crack tip also for stress singularity weaker than square-root.

The obtained results show that Mode II intersonic crack propagation in poroelastic fluid saturated materials can always occur within the regimes *i*) and *ii*). In particular, it can be observed from Fig. 2 that the Mode II stress and pore pressure singularity is lower than the square root within the intersonic regime *i*), namely $0 \leq \gamma_{II} < 0.5$, and that, for high porosity level, the exponent γ_{II} attains a maximum at an intermediate crack tip speed. Note that as n and, thus, ρ^w tend to vanish, then c_1 and c_w become unbounded, whereas c_2 and c_s tend to the longitudinal wave speed c_L for linear elastic materials. Therefore, in this limit the intersonic range *i*) approaches the supersonic regime $c > c_L$ for linear elastic materials, occurring with a non-singular stress field near the crack tip [5]. This solution is indeed recovered by the present approach, since the exponent γ is found to vanish as $n \rightarrow 0$. Within the regime *ii*), there exists for low porosity a special crack tip speed which is intermediate between c_3 and c_2 , such that the stress displays the square-root singularity, as it occurs for linear elastic material at $c = \sqrt{2} c_s$. Moreover, shear crack propagation within the regime *iii*) seems to be possible only for $c_2 < c < c^*$, where c^* denotes the crack tip speed corresponding to $\gamma_{II} = 0$, which depends on the porosity level.

Mode I intersonic crack propagation is found to be forbidden within the entire regimes *i*) and *ii*), since it should occur with a stress singularity stronger than square root ($\gamma_1 > 0.5$) and a negative energy release rate. Within the regime *iii*) Mode I crack propagation is forbidden for crack tip speeds lower than the limit speed c^* for intersonic Mode II crack propagation, but it may occur for $c^* < c < c_3$. In this favourable speed range, the exponent γ_1 of the Mode I stress and pore pressure singularity is found to range between 0 and 0.5.

For crack tip speeds belonging to regime *i*), the partial stress fields turn out to be discontinuous along two pairs of symmetric rays (Mach cones) emanating from the crack tip (see Fig. 1), whereas a single pair of these rays appears for the regimes *ii*) and *iii*). Note that in the present analysis of the near tip region the dissipative terms have been neglected. However, their contribution, which must be considered in a full-field investigation, may smooth the jump in the partial stress fields far from the crack tip.

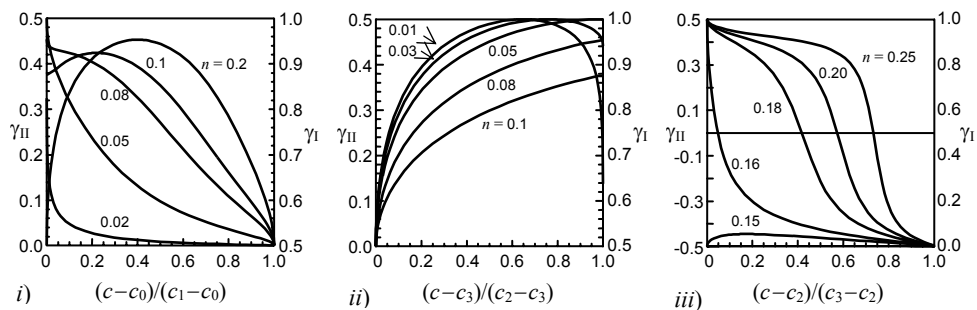


Fig. 2. Strength of the stress and pore pressure singularity under Mode I and Mode II as functions of the crack tip speed c ranging within the intersonic regimes *i*), *ii*) and *iii*) for Berea sandstone with permeable crack surfaces and different porosity levels.

REFERENCES

- [1] Atkinson C., Craster R.V., Plane strain fracture in poroelastic media. Proceedings of the Royal Society A, 434, 605-633 (1991).
- [2] Radi E., Bigoni D., Loret B., Steady crack-growth in elastic-plastic fluid-saturated porous media. International Journal of Plasticity, 18 (3), 345-358 (2002).
- [3] Loret B., Radi E., On dynamic crack growth in poroelastic fluid-saturated media. Journal of the Mechanics and Physics of Solids, 49 (5), 995-1020 (2001).
- [4] Freund L.B., Dynamic Fracture Mechanics; Cambridge University Press, Cambridge, 1990.
- [5] Broberg K.B., Cracks and Fracture, Academic Press, London, 1999.
- [6] Broberg K.B.: The near-tip field at high crack velocities. International Journal of Fracture, 39 (1-3), 1-13 (1989).
- [7] Liu C., Huang Y., Rosakis A.J., Shear dominated transonic interfacial crack growth in a bimaterial – II. Asymptotic fields and favourable velocity regimes. Journal of the Mechanics and Physics of Solids, 43 (2), 189-206 (1995).
- [8] Rosakis A.J., Samudrala O., Coker D., Cracks faster than the shear wave speed. Science, 284 (5418), 1337-1340 (1999).
- [9] Kubair D.V., Geubelle P.H., Huang Y.Y., Intersonic crack propagation in homogeneous media under shear-dominated loading: theoretical analysis. Journal of the Mechanics and Physics of Solids, 50 (8), 1547-1564 (2002).
- [10] Loret B., Harireche O., Acceleration waves, flutter instabilities and stationary discontinuities in inelastic porous media. Journal of the Mechanics and Physics of Solids, 39 (5), 569-606 (1991).